International Journal of Reliability, Risk and Safety: Theory and Application

Online ISSN: 2676-3346

Vol. 8/ Issue 2/ Year 2025/ pp. 11-21
DOI: 10.22034/IJRRS.2025.8.2.2
Received: 18 April 2025, Revised: 19 September 2025, Accepted: 20 September 2025
Available online at: https://www.ijrrs.com

Original Research Article

Detailed Seismic Risk Assessment of a Blast-Resistant Concrete Building

Sasan Motaghed [*1], Nasrollah Eftekhari [2], Ahmad Reza Fakhriyat [3], Heshmatollah Mahmoodian [4], and Masoud Dorfeshan [5]

1. Department of Civil Engineering, Faculty of Civil Engineering and Architecture, Shahid Chamran University of Ahvaz, Ahvaz, Iran

2. Faculty of Technology and Mining, Yasouj University, Choram, Iran

3. Center Of Monitoring Assessment and Prediction of Natural Disasters (MAP), Behbahan Khatam Alanbia University of Technology, Behbahan, Iran

4. Lorestan National University of Skills, Khorramabad, Iran

5. Department of Mechanical Engineering, Faculty of Engineering, Behbahan Khatam Alanbia University of Technology, Behbahan, Iran

*** motaghed@bkatu.ac.ir**

Abstract

Risk analysis plays a crucial role in pre-event planning by supporting informed decision-making and enabling effective strategies for crisis prevention and emergency response. This paper presents a comprehensive risk assessment of a specially designed concrete building with shear walls, engineered to withstand blast loads. Both deterministic seismic hazard analysis (DSHA) and non-extensive probabilistic seismic hazard analysis (NEPSHA) were conducted. The deterministic approach identified a peak ground acceleration (PGA) of 0.6g at the building site. NEPSHA estimated PGA values of 0.03g, 0.42g, and 0.74g for return periods of 10, 475, and 2,475 years, respectively. Hazard analysis results were visualized as hazard maps using GIS software. A three-story, blast-resistant concrete building with a 342-square-meter floor area and a shear wall lateral load-bearing system was modeled in OpenSees software. The structure's fragility curve was determined through incremental dynamic analysis (IDA), revealing a fundamental period of 0.08 seconds. The study quantified the probabilities of various damage levels at different hazard intensities and, using FEMA's Hazus methodology, estimated the resulting debris. Findings indicate that the shear wall-reinforced building, designed for blast resistance, satisfies the requirements for the design-level earthquake. However, its performance under severe and deterministic earthquake scenarios-particularly at the immediate occupancy performance level-warrants further investigation.

Keywords: Blast-Resistant Building; Petrochemical Facilities; Fragility Curve; Performance Level; Loss Estimation.

Nomenclature

APE	annual probability of exceedance
DSHA	deterministic seismic hazard analysis
GIS	geographic information system
GMPE	ground motion prediction equations
IO	immediate occupancy
IDA	incremental dynamic analysis
NEPSHA	non-extensive probabilistic seismic hazard analyses
PSHA	probabilistic seismic hazard analysis
PGA	peak ground acceleration
SCP	Sotolongo-Costa and Posadas
UHS	uniform hazard spectrum

1. Introduction

The safety of buildings against both natural and manufactured hazards is a major concern for engineers, homeowners, and facility managers. Seismic risk analysis is a well-established discipline focused on assessing the vulnerability of structures to earthquakes [1]. However, evaluating the resilience of buildings to blast effects is a relatively new and rapidly developing area of research [2]. Risk analysis involves identifying hazard factors that may cause damage (hazard identification), assessing the potential damage associated with these hazards (vulnerability), and evaluating the consequences resulting

How to cite this article:
S. Motaghed, N. Eftekhari, A.R. Fakhriyat, H. Mahmoodian, and M. Dorfeshan, "Detailed seismic risk assessment of a blast-resistant concrete building," *International Journal of Reliability, Risk and Safety: Theory and Application*, vol. 8, no. 2, pp. 11-21, 2025, doi: 10.22034/IJRRS.2025.8.2.2.

from the damage (exposure). [3,4]. Based on the results of risk analysis, analysts can decide what measures should be taken to eliminate or control potential damages or consequences. Hosseinpour et al. (2021) provided a comprehensive survey on seismic risk methods and their strengths and limitations [5]. Probabilistic procedures are an important category of the most widely used risk analysis methods. Traditionally, probabilistic seismic risk procedures rely on precise probabilistic models to quantify the uncertainties in structural demand and capacity [6,7] and to estimate the probability of structural failure [8-10].

With ongoing industrial development and the heightened risk of explosions, there is a growing emphasis on explosion-resistant buildings, particularly within critical industries. These structures are gaining increased attention as crucial measures for safety and risk reduction [11]. These buildings are designed to withstand the effects of unexpected explosions (such as process explosions) or intentional explosions (such as war or terrorist attacks). Typically, buildings designed to withstand medium to high blast pressures use in-situ concrete walls. In such structures, the thickness of the concrete walls, along with the size and placement of the reinforcing bars, must be carefully chosen to ensure adequate blast resistance. The minimum thickness for in-situ reinforced concrete walls is 200 mm.

Explosions are highly likely in petrochemical facilities, such as gas refineries. Therefore, the design of blast-resistant structures is vital to minimize human fatalities and damage to facilities in petrochemical plants [12]. The admissible structural damage level induced in blast design for petrochemical plants is determined according to the owner's blast protection philosophy [13]. Therefore, structures in gas refineries exhibit varying levels of safety against loads caused by events, depending on the hazard sources and the design philosophy [14]. The question is how a building designed to withstand the effects of the explosion will behave against the seismic loads. In this paper, this issue was considered using a case study.

ElSayed et al. (2016) evaluate the resilience of seismically detailed reinforced concrete-block shear walls under blast loads. They emphasize the dual role of seismic detailing in enhancing both earthquake and blast performance. Their findings suggest that incorporating seismic detailing significantly improves the structural resilience and damage tolerance of shear walls subjected to blast effects, making them suitable for critical infrastructure protection.

Shi et al. (2023) conduct a reliability analysis of reinforced concrete columns under combined seismic and blast loads, addressing the complex interaction between these hazards. Their probabilistic approach accounts for uncertainties in loading and material properties, providing insights into the structural safety margins when subjected to simultaneous seismic and blast events.

Keertan et al. (2023) analyze structural responses under both types of seismic and blast extreme events. The research identifies differences in failure modes and performance criteria, highlighting the need for tailored design strategies for blast versus seismic resistance.

Several countries have adopted Hazus, a standardized methodology developed by FEMA, to evaluate potential losses from natural hazards such as earthquakes [18-19]. Hazus combines engineering principles with mathematical modeling, utilizing GIS technology to estimate both structural and non-structural damages, as well as the associated economic and social impacts [20]. This approach has been applied in seismic risk analyses for bridges [21], urban areas [22], and reinforced concrete structures [23]. This paper presents a detailed seismic risk assessment of a blast-resistant, three-story concrete building featuring multiple shear walls. Located within a gas refinery, the building is specifically designed to withstand explosion loads, making it significantly stronger than typical structures. As a result, standard fragility curves are not applicable, necessitating the development of a tailored fragility curve for this building. To achieve this, the structure is modeled using OpenSees software, and its specific fragility curve is derived through incremental dynamic analysis (IDA). Both deterministic and non-extensive probabilistic seismic hazard analyses (NEPSHA) are conducted, from which estimates of damage, debris generation, and casualties are obtained. The study aims to assess the resilience of reinforced masonry shear wall systems under blast conditions, providing valuable insights to inform the design and construction of blast-resistant buildings.

2. Methodology

Risk analysis means finding the consequences of an event. Risk analysis consists of three components: hazard, vulnerability, and exposure, as shown in Figure 1. The result of this process is determining the probabilities of the considered outcomes of the intended hazard.

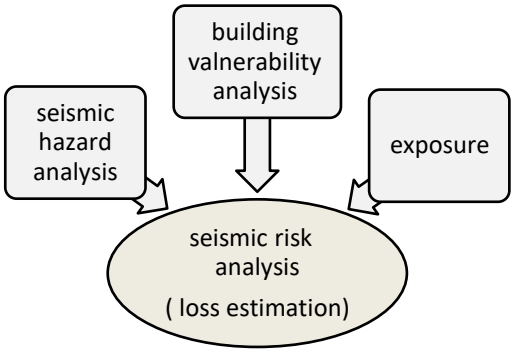

Figure 1. Seismic risk components

The first step in risk analysis is hazard analysis [24-25-26]. The hazard analysis can be done using deterministic (DSHA) and probabilistic methods. In this paper, the deterministic and non-extensive probabilistic seismic hazard analysis (NEPSHA) is used. In NEPSHA, the recurrence of earthquakes is based on the SCP law, which is based on the physics of the events [27-28-29].

The second step of risk analysis is assessing the vulnerability of the structure [14-30-31]. There are several classifications of damage criteria to describe building damage from different perspectives [32-33,23-24]. Karim Zadeh et al. (2022) conducted a comprehensive study on the types of buildings in Iran. Due to the differences between national design codes, construction practices, and building materials, it is common to develop general fragility functions for the different types of typical buildings constructed in each region. They classified the typical Iranian buildings into 35 categories based on materials, load-bearing system, age, height, and level of code [34]. These types of curves are beneficial for assessing approximate vulnerability or for examining large areas. In conducting a detailed assessment of a building, it is essential to develop a specific fragility curve tailored to that structure. In this paper, using the OpenSees software, based on the results of incremental dynamic analysis, the fragility curve of the concrete shear wall building is presented. We consider four damage criteria, which correspond to minor, moderate, extensive, and complete damage levels based on the recommendations of previous studies. These limit states are defined based on the yield and ultimate displacement of the system. Here, the limit states related to the damage criteria defined for this study are described in Table 1 [34].

According to Table 1, a limit state is reached when the structure's maximum displacement attains its specified displacement values. For example, if the maximum displacement of the structure reaches $0.75\times S_{d_y}$, the structure has reached the LS1 damage state.

Table 1. Structural limit states descriptions

Limit state	Description	Displacement
LS1	Minor damage	$0.75\times S_{d_y}$
LS2	Moderate damage	$0.5\times S_{d_y} + 0.33\times S_{d_u}$
LS3	Moderate damage	$0.25\times S_{d_y} + 0.67\times S_{d_u}$
LS4	Full damage	S_{d_u}

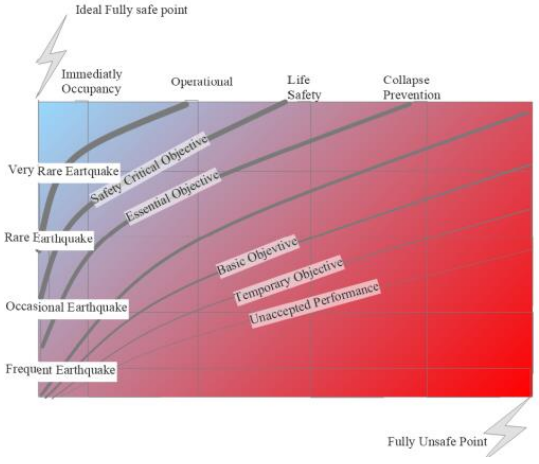

Figure 2. Relationship between performance levels and structural damage levels in different earthquake levels

Based on the damage limit status (LS1 to LS4), different performance levels of the structure can be determined. Intuitively, the relationship between damage limit status and performance levels is shown in Figure 2. Also, in this figure, the relationship between the performance and damage of the structure with the concrete cracking, steel bars yield point, and the element ultimate capacity point of the structure is shown [35].

Using this information, the structure's performance during an earthquake can be evaluated. Using the building damage and performance data, the Hazus method can estimate the amount of debris and casualties. For this purpose, the unit weight (weight per unit area) of the building (Table 2) and the debris volume (Table 3) are required.

Table 2. Unit weight (in kilograms per square meters) updated based on building information (HAZUS 1999)

Reinforced concrete and steel		Break, wood, and others	
Non-Structural	Structural	Non-Structural	Structural
43	1055	57	0

Table 3. The debris produced from the damaged structural and non-structural parts (in percent weight) for the high-code concrete shear wall building (HAZUS 1999)

Debries type		Break and wood	Reinforced concrete and steel
Structural damages	minor	0	1
	moderate	0	7
	extensive	0	35
	Complete	100	100
Non-Structural damages	minor	0	0
	moderate	5	8
	extensive	33	28
	Complete	100	100

In this way, the probability of debris production can be calculated by multiplying the likelihood of damage (obtained in the previous step), the unit weight (Table 2), and the percentage of debris (Table 3) as:

Probability of debris = probability of damage × unit weight ×percentage of debris

Here, the unit weight shows the weight of materials per unit area of the building.

3. Seismic hazard analysis

The study building is located in a Gas Refining Company (BBGRC). The map of active faults (Figure 3) shows that the BBGRC is situated in the seismic zone. The survey of the earthquakes in the region also shows the high seismic activity of the area. The most significant faults in the region are listed in Table 4.

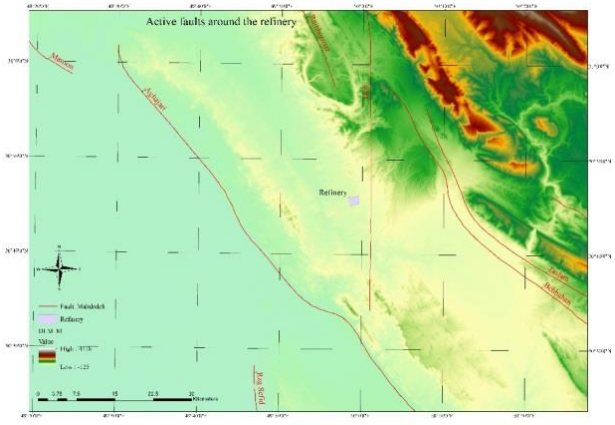

Figure 3. Active faults around the BBGRC

Based on this visual information, the hazard analysis is carried out using both deterministic and probabilistic approaches. Fault information, including the maximum magnitude (M_{max}) and distance (R), are given in Table 4.

Table 4. Faults around BBGRC

fault	M_{max}	Length (km)	Nearest Distance to site (km)
Behbahan	7.35	78.8	8.4
Tashan	7.26	65.2	11.0
Izeh	7.77	192.7	21.1
Aghajari	7.52	113.1	23.7
Baba Khaneh	6.69	19.3	24.0
Mishan	7.40	87.2	28.7
Rag Sefid	7.52	113.5	44.7
Ramhormoz	7.87	237.2	49.4
M. F. F	7.44	95.9	71.2
Lahbari	7.89	249.0	76.1
M.F	6.69	19.4	81.8
Kuh-e Noh	6.80	24.6	82.0
Maroon	6.86	27.7	90.3
Sivak	7.09	45.4	94.4
M.F	6.71	20.1	97.6
Jarreh	6.93	32.4	100.3
Seh Paran	6.58	15.3	102.4
Mangasht	6.73	21.3	109.5
Shah Neshin	6.86	27.6	109.5
Dena	7.48	104.4	112.9
Mordehfel	7.13	49.9	115.5
Cheshmeh Chenar	6.71	20.2	122.1
Sarakan-e Bala	6.72	20.8	123.2
Massan	7.38	83.7	124.0
Kazerun	7.56	123.2	124.4
Bazoft	7.04	40.9	125.8
Ahvaz	7.51	110.7	126.7
Kermani	7.00	37.6	127.3
noname	7.08	44.6	127.3
Chal Kalagh	7.09	45.8	130.5
Ab-e Rak	6.61	16.6	133.5
Dopolan	7.25	64.0	134.8
Kuh Siah	7.31	71.7	135.1
Bideh	6.94	33.2	135.3
Sabzeh Kuh	7.18	54.7	137.7
Ahvaz	6.61	16.3	138.8
Taveh Siah	6.65	17.9	139.0
Farum	6.57	15.0	140.5
Kordan	6.96	34.2	141.5
Borazjan	7.76	185.9	143.0
Avafi	6.57	15.1	147.6
Kakan	6.70	20.0	149.1
M.F	6.93	32.7	149.4
Mourchegan	6.91	31.1	149.7
H. Z	7.37	82.2	151.5
Semirom	6.90	30.1	152.5
Ardal	7.78	195.4	153.7
noname	7.22	59.8	154.5
Masjed Soleiman	6.95	33.7	158.6
Janga	6.94	33.1	159.2
Hana	6.80	24.7	159.6
Zard Kuh	7.85	227.5	160.8
Kuhe-eAqdagh	6.88	29.1	161.0
M.Z.R	7.54	119.0	161.0
M.Z.R	7.04	40.8	163.2
Mafarun	7.32	74.2	163.5
M.Z.R	7.10	46.4	168.3
M.Z.R	7.80	204.3	168.9
Andakan	7.18	54.5	173.4
Solaghan	7.60	132.9	180.1
Karehbas	7.56	122.7	180.3
noname	6.39	10.3	181.6
Dasht-e Gol	6.71	20.3	182.7
Qalat	7.08	44.6	184.2
Shahr-e Kord	7.67	154.2	185.8
Susan	6.69	19.5	185.9
Kelestan	7.14	50.4	187.1
M.F	7.44	96.0	187.7
Noname	6.70	20.0	187.9
Chal-e Munar	6.60	16.1	193.4
Katah	7.45	96.8	193.6
Cher cher	6.95	33.6	198.2
Z. F. F	7.61	136.2	199.2

3.1 Deterministic seismic hazard analysis (DSHA)

The ruptures of Behbahan, Tashan, Aghajari, and Izeh faults are considered as DSHA earthquake scenarios. Information on these faults is given in Table 4. Figure 3 shows the location of these faults around the site.

Ghasemi et al. (2009) attenuation relationship is given below [36]. This relationship is presented for Iran and the Middle East, for Mw = (5.0-7.4), R_{rup} & R_{hyp} distances. This relationship is particularly suitable for this region [37].

The functional form of the relationship is as follows:

$$Log_{10}\, Sa = a_1 + a_2M + a_3 \log10(R + a_4 10^{\,a_5M}) + a_6S1 + a_7S2$$

The a1 to a5 and R1 and R2 parameters for 17 periods are given in Ghasemi et al., 2009[36].

Based on the DSHA calculation, the uniform hazard spectrum (UHS) for four faults near the site is given in Figure 4. Based on the results, the most dangerous fault around the refinery is the Izeh fault due to its very short distance to the site. This fault with a length of nearly 200 km can produce an earthquake with a magnitude of about 7.73 Mw. This earthquake can create PGA 0.6g at the site. This PGA is about twice the standard No. 2800 PGA value for the site. Other faults produce PGAs near the value of the standard No. 2800.

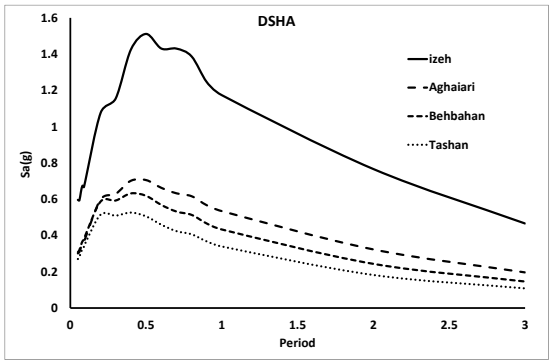

Figure 4. DSHA Uniform hazard spectrum (UHS)

3.2 Non-extensive probabilistic seismic hazard analysis (NEPSHA)

Based on the standard No. 2800, NEPSHA for three exceedance probabilities of 99.5, 10, and 2% in 50 years has been obtained using Open Quick software and MATLAB code.

The seismicity parameters of the area include a and q values of the SCP relation are 0.00108 and 1.65, respectively [24]. The tapered minimum magnitude is 4.5-5.5 [38], and the maximum magnitude is selected based on Table 4. In NEPSHA, the attenuation relationships of Akkar and Kagnan 2020 (0.2), Akkar et al. 2014 (0.35), Chiou and Youngs 2008 (0.35), and Zhao et al. (2006) (0.1) have been used [39-42].

Figure 5 shows the NEPSHA map for the 10-year return period (99.5% probability of exceeding in 50 years), Figure 6 shows the NEPSHA map for the 475-year return period (10% probability of exceedance in 50 years), and Figure 7 shows the NEPSHA map for the return period of 2475 years (2% probability of exceedance in 50 years). According to these figures, the earthquake PGA at the site for return periods of 10, 475, and 2475 years is 0.03 g, 0.42 g, and 0.74 g, respectively. Comparing these values with the standard No. 2800 shows that this area has a more than standard No. 2800 (that is, 0.3g for a return period of 10% in 50 years).

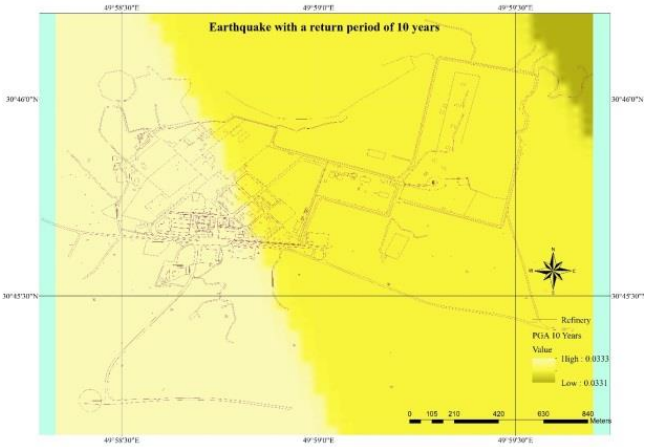

Figure 5. NEPSHA map of the 10-year return period (APE=0.1)

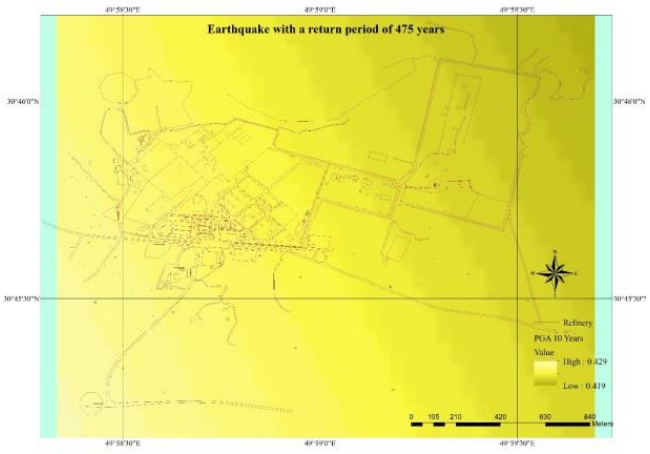

Figure 6. NEPSHA map of the 475-year return period (APE=0.0021)

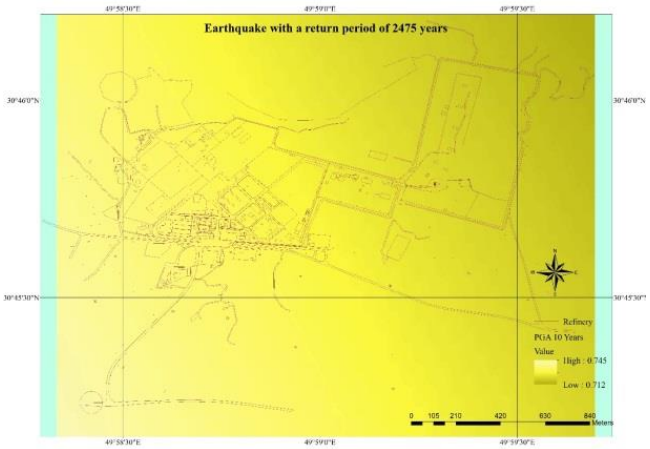

Figure 7. NEPSHA map of the return period of the 2475-year (APE=0.0004)

4. Building information, fragility, and seismic risk

The Administration building of BBGRC has been modeled and analyzed as a case study. This building was designed based on ASCE for blast loading [43]. The geometry, configuration, and structural information of the building are shown in Figures 8, 9, 10, and 11. This three-story building is 10 m height, and 342 m2 floor area. The lateral bearing system of the building is a dual system composed of RC moment-resisting frames (MRFs) and RC shear walls. As can be seen from Figure 8 (building plan), in each direction, the shear walls are attached along with the moment-resisting frame. The details of the modeling of this structure in terms of uncertainty can be obtained from the references [44-46]. The selected frame in axis 3 of the building is shown in Figure 9. Figure 10 shows a section of the typical shear wall. Figure 11 shows the building elevation.

The 3-story building is located in the˝39´45°30 North and˝49´58°49 East. This building was constructed in 2010 and is considered to have average compliance

with regulations. The effects of the infill masonry frame on the structural behavior have been neglected. The location of this building is shown in Figure 12. Structural elements information is given in Tables 5, 6, and 7.

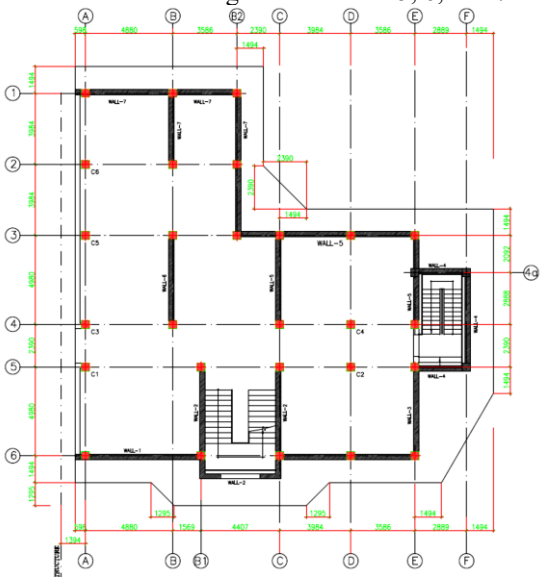

Figure 8. Typical floor plan of the Administration building

Fragility curves describe the probability of damage to a building. The damage relates to the structural system, drift-sensitive non-structural components, and acceleration-sensitive non-structural components (and contents). For a given level of building response, fragility curves describe damage between four physical damage states: minor, moderate, extensive, and complete.

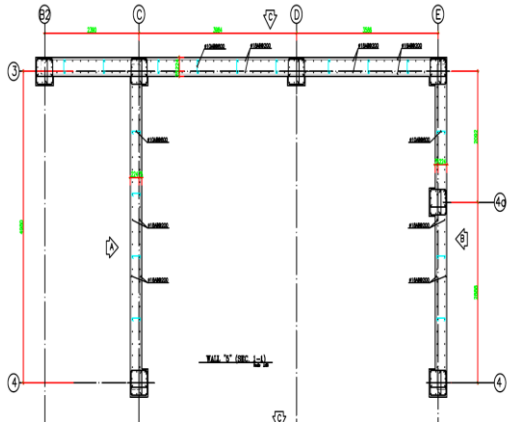

Figure 9. Elevation of the studied building

Table 5. Shear wall boundary element information

dimensions	Longitudinal Steel bars	transversal Steel bars
450×450(mm)	12Φ20 (mm)	Φ18@200 (mm)

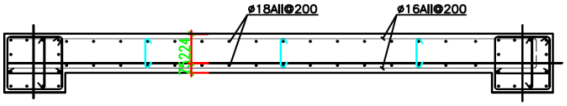

Figure 10. Shear wall section

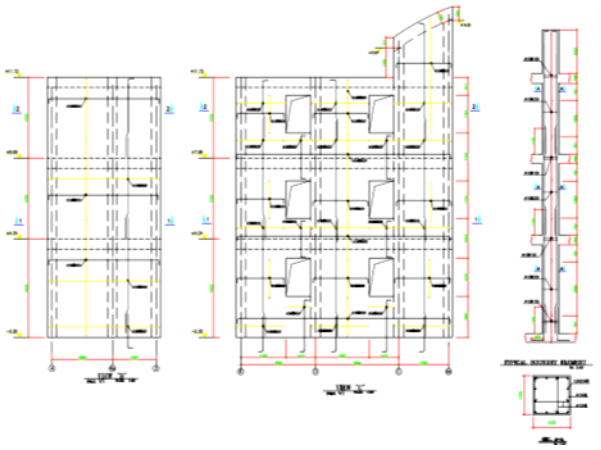

Figure 11. Administration building elevation

Table 6. Shear wall web information

Levels	Width (mm)	Top Steel	Bottom Steel	Reinforcing ratio in the horizontal direction	Reinforcing ratio in the vertical direction
1	300	Φ18@200	Φ18@200	0.0067	0.0085
2	300	Φ18@200	Φ18@200	0.0067	0.0085
3	300	Φ18@200	Φ18@200	0.0067	0.0085

Table 7. Moment resisting reinforced concrete frame information

Story	Exterior Columns		Interior Columns		Beams			
	Size mm	Steel	Size mm	Steel	Size mm	Top Steel	Bottom Steel	Int Steel
1	450×450	12Φ20	716×716	12Φ20	1120×710	3Φ22	3Φ22	2Φ14
2	450×450	12Φ18	716×716	12Φ20	1120×710	3Φ22	3Φ22	2Φ14
3	450×450	12Φ18	716×716	12Φ20	1070×660	3Φ22	3Φ22	2Φ14

The fragility curve is a graph that shows the probability of a certain level of damage in the structure as a function of the intensity of ground motion (for example, spectral acceleration or maximum ground acceleration). This curve is useful for predicting the probability of damage in a specific structure under different levels of ground motion.

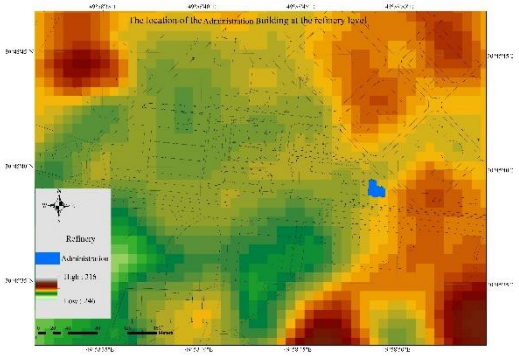

Figure 12. The location of the Administration building in the BBGRC

Incremental dynamic analysis (IDA) is a method used in earthquake engineering to investigate the seismic performance of a structure. This method involves subjecting the structure to a series of seismic loads, with

the intensity of each load gradually increasing until the structure's performance objectives are achieved. Considering that static analysis is associated with ignoring dynamic effects and duration effects, the answer of time history analysis, as a time domain analysis, is more favorable to determine the response of the structure.

The choice of ground motion records strongly influences the results of time history analysis. By performing nonlinear dynamic response history analyses using a suite of different ground motion records, it is possible to estimate uncertainties within a probabilistic framework. In this context, Incremental Dynamic Analysis (IDA) is employed to generate fragility curves for structures, which effectively account for various seismic input uncertainties-including magnitude, distance, and frequency content variability. We used 22 pairs of ground motion records for IDA analysis based on FEMA P695. The conditional mean spectrum (CMS) method, proposed by Baker and Cornell [47], is used for record selection [45]. Each pair contains two horizontal components of an earthquake at a recording station. Specifications of the 44 ground motion records (2×22) are shown in Table 8. The UHS of severe, design, and service earthquakes in the location of the Administration building are shown in Figure 13.

Figure 14 shows the fragility curves of the structure. The fragility curves show the probability distribution of different damage intensities in the four performance levels of the structure, which include minor, moderate damage, extensive, and complete damage. As it is known, this curve shows the probability of occurrence of a certain level of damage for different values of spectral acceleration (S_a).

Table 8. Earthquakes (EQ) used in IDA

EQ ID	Earthquake Information			Recording Station	
	M	Year	Name	Name	Owner
1	6.	199	Northridge	Beverly Hills -	USC
2	6.	199	Northridge	Canyon Country-	USC
3	7.	199	Duzce, Turkey	Bolu	ERD
4	7.	199	Hector Mine	Hector	SCSN
5	6.	197	Imperial Valley	Delta	UNAMUCS
6	6.	197	Imperial Valley	El Centro Array #11	USGS
7	6.	199	Kobe, Japan	Nishi-Akashi	CUE
8	6.	199	Kobe, Japan	Shin-Osaka	CUE
9	7.	199	Kocaeli, Turkey	Duzce	ERD
10	7.	199	Kocaeli, Turkey	Arcelik	KOERI
11	7.	199	Landers	Yermo Fire Station	CDMG
12	7.	199	Landers	Coolwater	SCE
13	6.	198	Loma Prieta	Capitola	CDMG
14	6.	198	Loma Prieta	Gilroy Array #3	CDMG
15	7.	199	Manjil, Iran	Abbar	BHRC
16	6.	198	Superstition	El Centro Imp. Co.	CDMG
17	6.	198	Superstition	Poe Road (temp)	USGS
18	7.	199	Cape Mendocino	Rio Dell Overpass	CDMG
19	7.	199	Chi-Chi, Taiwan	CHY101	CWB
20	7.	199	Chi-Chi, Taiwan	TCU045	CWB
21	6.	197	San Fernando	LA - ollywood Stor	CDMG
22	6.	197	Friuli, Italy	Tolmezzo	--

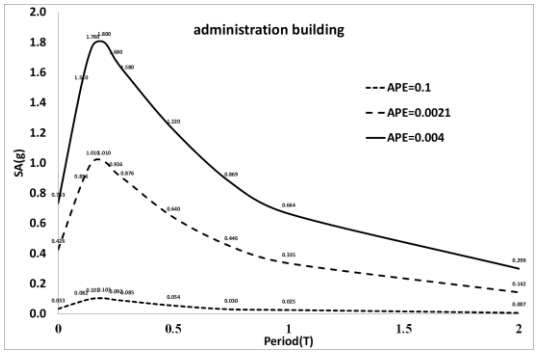

Figure 13. The UHS of severe, design, and service earthquakes in the location of the Administration building

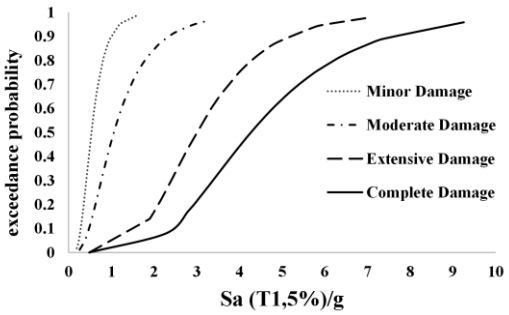

Figure 14. Fragility curves for different damage statuses (minor, moderate, extensive, and complete) for the administration building

Table 9. Probability of exceeding different levels of damage in deterministic, severe, design, and service earthquakes at the building

hazard	Performance level			
	LS1	LS2	LS3	LS4
Deterministic	89	69	10	3
APE=0.004	99	73	12	4
APE=0.021	82	34	3	1
APE=0.1	4	1	0	0

According to the value of S_A(T=0.08s), the probability values of minor, moderate, extensive, and complete damage in the Administration building are extracted based on Figure 14 and summarized in Table 9.

According to Table 9, the probability of complete and extensive damage to the building in an earthquake is very low. Most likely, the building will suffer slight damage in the design earthquake, but there is also the probability of moderate damage. In deterministic and severe earthquakes, the likelihood of moderate damage is about 70%, which is significant.

In this way, it can be seen that blast design is not a sufficient guarantee to have a suitable seismic performance at all performance levels. Especially in an area with relatively high seismic hazard, it is necessary to pay attention to the issue of seismic design independent of the blasting design, especially at the immediate occupancy (IO) performance level.

This finding is consistent with seismic design codes, which require all buildings-including those primarily designed for other forces such as wind-to meet seismic and ductility criteria. Accordingly, it is necessary to carry

out seismic retrofitting for the mentioned structure in accordance with the latest edition of the relevant design code.

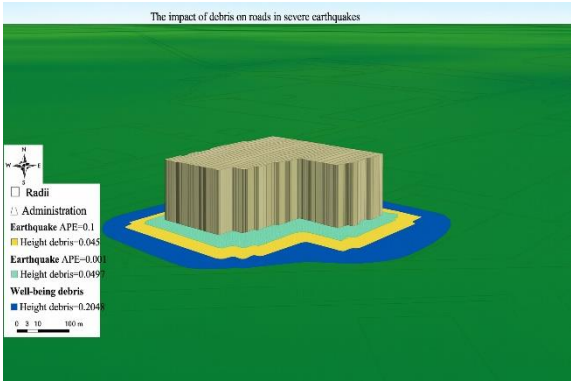

Figure 15. The impact of debris on roads in severe earthquakes

With the damage probabilities determined, the amount of debris and casualties can now be estimated using the Hazus method. The weight of materials per square area (Table 2), the debris produced from the damaged parts (Table 3), and the debris unit weights are used for debris volume calculation.

In a severe earthquake, the amount of debris is estimated at 107.73 tons, which results in 10% of the road being closed; therefore, vehicle traffic is not significantly impacted.

Accounting for the 25 occupants in the administration building, the number of casualties in the severe earthquake is 2.5 people, and about 1.25 people are also trapped. At night, there are 5 people in the building, and 1 person may be injured in a severe earthquake. The debris produced is shown in Figure 15. It is important to note that the Hazus methodology employs a deterministic framework in this context; however, the number of casualties may vary probabilistically with changes in the number of occupants in the building, a factor that has not been considered in this study.

It should be noted that the Administration building is the most important in the refinery and serves as the central hub for all decision-making during and after a crisis. Therefore, the building's IO performance is critical and is considered essential for ensuring public safety.

This study inevitably faces some limitations, primarily concerning the seismic hazard analysis, accessibility of building-specific data, and the assumptions inherent in both Hazus and OpenSees methodologies. In the hazard analysis, the use of both DSHA and NEPSHA significantly helped reduce uncertainty. Nevertheless, limitations remain due to inevitable simplifications, such as the reliance on available regional seismicity data, assumptions in modelling earthquake recurrence, and GMPE. On the building side, limited access to detailed as-built information- such as material properties, reinforcement detailing, and the effect of infill walls (which were neglected in the OpenSees model)-introduces additional uncertainty. The Hazus methodology, though widely accepted, is fundamentally based on generalized fragility, debris, and casualty relationships that may not fully reflect the specialized nature of a blast-resistant building; so, while customized fragility curves were generated by incremental dynamic analysis, some reliance on standard assumptions persists. Despite these challenges, the study attempted to mitigate limitations through best-practice methods (e.g., NEPSHA, structure-specific fragility development, and updated exposure data) to ensure that risk assessment results are as robust and site-relevant as possible. Further advances could be achieved with more detailed building data and by including additional sources of modeling uncertainty.

5. Conclusion

A common and critical inquiry among managers and engineers responsible for facilities designed in previous years to resist blast effects is whether these buildings also meet current seismic code requirements, and to what extent they can withstand earthquake forces according to the latest standards. In this paper, we are looking for an answer to this question in a real structure that was built in 2010 in a gas refinery. To answer this question, a complete process of earthquake risk analysis, including deterministic and non-extensive probabilistic hazard analysis, extraction of fragility curves, and damage assessment, has been carried out with the most up-to-date methods.

Based on the results, the probability of complete and extensive damage to the building in an earthquake is very low. Most likely, the building will suffer slight damage in the design earthquake, but there is also the probability of moderate damage. In deterministic and severe earthquakes, the probability of moderate damage is about 70%, which is significant. In this way, it can be seen that blasting design is not a sufficient guarantee to have a suitable seismic performance at all performance levels. Especially in an area with relatively high seismic hazard, it is necessary to pay attention to the issue of seismic design independent of the blasting design, especially at the immediate occupancy (IO) performance level**.**

For a more detailed discussion on this subject, we need to know that seismic design prioritizes ductility, energy dissipation, and the ability for structures to undergo controlled, global deformations without collapse, with measures such as shear walls, moment-resisting frames, and energy dissipaters being standard. In contrast, blast design focuses on enhancing initial stiffness, local reinforcement, and the capacity to absorb and withstand impulsive, high-frequency loads, often employing sacrificial elements and specialized materials like ultra-high-performance concrete and fiber-reinforced polymers to prevent sudden localized failures. These differing emphases mean that buildings optimized solely for blast loading may lack the adequate global ductility required for seismic resilience. Retrofitting strategies to

bridge this gap include introducing or enhancing seismic energy dissipation devices, such as viscous or friction dampers, base isolators, and supplementary bracing systems, while retaining or upgrading local strengthening measures initially intended for blast resistance, including composite wrapping and shock-mitigating layers.

This study involves several assumptions and inherent limitations that affect the interpretation of the results. A notable modeling simplification is the neglect of infill walls in the structural analysis. Additionally, uncertainties remain in the seismic hazard characterization due to reliance on available regional seismicity data, ground motion prediction equations, and recurrence models. Material properties and reinforcement details were based on limited access to as-built documentation, which may further affect the accuracy of the modeled structural behavior. The Hazus methodology used for damage and casualty estimation, while widely accepted, is fundamentally based on generalized fragility and debris relationships that may not fully capture the unique performance of blast-resistant structures designed with enhanced stiffness and strength. These factors collectively restrict the generalizability of the findings.

Acknowledgments

The research team expresses gratitude to Bid-Boland Gas Refinery Company for their support. Also, we thank the Center of Monitoring, Assessment, and Prediction of natural disasters (MAP) of Behbahan Khatam Alanbia University of Technology.

Conflict of Interests

No conflict of interest has been expressed by the authors.

6. References

[1] Federal Emergency Management Agency (FEMA), "Hazus-MH MR4 technical manual, multi-hazard loss estimation methodology earthquake model," FEMA 366, Washington, DC, 2003.

[2] M. Z. Kangda, "Blast protection techniques: A review," *Archives of Computational Methods in Engineering*, vol. 29, no. 5, pp. 3509–3529, 2022, https://doi.org/10.1007/s11831-021-09704-5.

[3] S. Motaghed, H. Mahmoodian, and S. Dehdari, "Case studies in seismic risk assessment of masonry fire station buildings," *International Journal of Reliability, Risk and Safety: Theory and Application*, vol. 7, no. 2, pp. 40-51, 2024, https://doi.org/10.22034/IJRRS.2024.7.2.4.

[4] S. Motaghed, N. Eftekhari, A. Nakhlian, L. Emadali, and H. Mahmoudian, "Seismic risk analysis in the Behbahan city old fabric," *Journal of Safe City*, vol. 8, no. 3, pp. 1-25, 2024, (in Persian), https://doi.org/10.22034/ispdrc.2024.2035043.1119.

[5] V. Hosseinpour, A. Saeidi, M. J. Nollet, and M. Nastev, "Seismic loss estimation software: A comprehensive review of risk assessment steps, software development and limitations," *Engineering Structures*, vol. 232, 2021, Art. no. 111866, https://doi.org/10.1016/j.engstruct.2021.111866.

[6] A. Nicknam, M. Khanzadi, S. Motaghed, and A. Yazdani, "Applying b-value variation to seismic hazard analysis using closed-form joint probability distribution," *Journal of Vibroengineering*, vol. 16, no. 3, pp. 1376-1386, 2014.

[7] M. Khanzadi, A. Nicknam, A. Yazdani, and S. Motaghed, "A Bayesian approach for seismic recurrence parameters estimation," *Journal of Vibroengineering*, vol. 16, no. 2, pp. 977-986, 2014.

[8] D. W. Jia and Z. Y. Wu, "Seismic risk analysis based on imprecise distribution and failure probability function under multidimensional limit state," *Structures*, vol. 50, pp. 963–977, 2023, https://doi.org/10.1016/j.istruc.2023.02.036.

[9] M.Erdik, "Earthquake risk assessment," *Bulletin of Earthquake Engineering*, vol. 15, no.12 pp. 5055–5092, 2017, https://doi.org/10.1007/s10518-017-0235-2.

[10] F. C. Ponzo et al., "Advanced modelling and risk analysis of RC buildings with sliding isolation systems designed by the Italian seismic code," *Applied Sciences*, vol. 11, no. 4, p. 1938, 2021, https://doi.org/10.3390/app11041938.

[11] S. M. H. Khatami and H. Momenabadi, "A full coupled numerical method for dynamic response of metro tunnel subjected to surface explosion," *Journal of Rehabilitation in Civil Engineering*, vol. 10, no. 3, pp. 21-36, 2022, https://doi.org/10.22075/jrce.2021.23198.1501.

[12] O. Bedair, "Economical damage classification approach for blast-resistant buildings in petrochemical plants," *Practice Periodical on Structural Design and Construction*, vol. 25, no. 3, 2020, https://doi.org/10.1061/(asce)sc.1943-5576.0000503.

[13] Task Committee on Blast-Resistant Design of the Petrochemical Committee of the Energy Division of ASCE, Design of blast-resistant buildings in petrochemical facilities, American Society of Civil Engineers, 2010.

[14] Abdollahzadeh, G., Faghihmaleki, H. "Proposal of a probabilistic assessment of structural collapse concomitantly subject to earthquake and gas explosion," *Frontiers of Structural and Civil Engineering,* vol. 12, pp. 425–437, 2018, https://doi.org/10.1007/s11709-017-0427-5.

[15] M. ElSayed, W. El-Dakhakhni, and M. Tait, "Resilience evaluation of seismically detailed reinforced concrete-block shear walls for blast-risk assessment," *Journal of Performance of Constructed Facilities*, vol. 30, no. 4, 2016, Art. no. 04015087, https://doi.org/10.1061/(ASCE)CF.1943-5509.0000742.

[16] X. Shi, X. Sun, and J. Cui, "Reliability analysis of reinforced concrete columns under combined seismic and blast loads," *Science China Technological Sciences*, vol. 66, no. 2, pp. 363–377, 2023, https://doi.org/10.1007/s11431-022-2265-5.

[17] T. S. Keertan, T. M. Priya, and J. Bommisetty, "Comparative study on RCC frames subjected to blast and earthquake loading," *Materials Today: Proceedings*, 2023, https://doi.org/10.1016/j.matpr.2023.05.334.

[18] M. Nastev, "Adapting Hazus for seismic risk assessment in Canada," *Canadian Geotechnical Journal*, vol. 51, no 2, pp. 217–222, 2014, https://doi.org/10/1139/cgj-2013-0080.

[19] Federal Emergency Management Agency (FEMA), Hazus Multi-Hazard Loss Estimation Methodology: Earthquake Model (Hazus®-MH Technical Manual 2.1), Washington, DC: Mitigation Division, Department of Homeland Security, FEMA, 2012.

[20] C. A. Kircher, R. V. Whitman, and W. T. Holmes, "Hazus earthquake loss estimation methods," *Natural Hazards Review*, vol. 7, no. 2, pp. 45–59, 2006, https://doi.org/10.1061/(asce)1527-6988(2006)7:2(45).

[21] S. Mangalathu, F. Soleimani, and J. S. Jeon, "Bridge classes for regional seismic risk assessment: Improving Hazus models," *Engineering Structures*, vol. 148, pp. 755–766, 2017, https://doi.org/10.1016/j.engstruct.2017.07.019.

[22] A. Badawy, I. Korrat, M. El-Hadidy, and H. Gaber, "Update earthquake risk assessment in Cairo, Egypt," *Journal of Seismology*, vol. 21, no. 4, pp. 571–589, 2016, https://doi.org/10.1007/s10950-016-9621-5.

[23] A. Melani, R. Khare, R. Dhakal, and J. Mander, "Seismic risk assessment of low rise RC frame structure," *Structures*, vol. 5, pp. 13–22, 2016, https://doi.org/10.1016/j.istruc.2015.07.003.

[24] A. Yazdani, A. Nicknam, M. Khanzadi, and S. Motaghed, "An artificial statistical method to estimate seismicity parameter from incomplete earthquake catalogs: A case study in metropolitan Tehran, Iran," *Scientia Iranica*, vol. 22, no. 2, pp. 400-409, 2015, https://scientiairanica.sharif.edu/article_1874.html.

[25] S. Motaghed, N. Eftekhari, M. Mohammadi, and M. Khazaee, "Logic tree branches' weights in the probabilistic seismic hazard analysis: The need to combine inter-subjective and propensity probability interpretations," *Journal of Seismology*, vol. 27, pp. 1035–1046, 2023, https://doi.org/10.1007/s10950-023-10177-1.

[26] S. Motaghed and A. Fakhriyat, "A Reliable Method for Determining the tapered minimum magnitude in a probabilistic seismic hazard analysis," *International Journal of Reliability, Risk and Safety: Theory and Application*, vol. 5, no. 2, pp. 89–95, 2023, https://doi.org/10.30699/ijrrs.5.2.9.

[27] S. Motaghed, M. Khazaee, N. Eftekhari, and M. Mohammadi, "A non-extensive approach to probabilistic seismic hazard analysis," *Natural Hazards and Earth System Sciences*, vol. 23, no. 3, pp. 1117–1124, 2023, https://doi.org/10.5194/nhess-23-1117-2023.

[28] S. Motaghed, A. Nakhlian, L. Emadali, N. Eftekhari, and H. Mahmoudian, "Seismic hazard assessment using arithmetic-weighted overlay method based on earthquake potential index (EPI), the southwestern Iran," *Iranian Journal of Remote Sensing & GIS*, vol. 17, no. 1, pp. 23-40, 2025, (in Persian), https://doi.org/10.48308/gisj.2023.229646.1133.

[29] S. Motaghed et al., "Reliability of Iranian existing residential reinforced concrete structures in seismic events," *International Journal of Reliability, Risk and Safety: Theory and Application*, vol. 6, no. 2, pp. 55–64, 2023, https://doi.org/10.22034/ijrrs.2023.6.2.7.

[30] M. Donà, G. Piredda, A. Zonta, E. Bernardi, and F. da Porto, "Seismic fragility of unbraced industrial steel pallet racks," *Structural Safety*, vol. 110, 2024, Art. no. 102497, https://doi.org/10.1016/j.strusafe.2024.102497.

[31] S. Motaghed, M. S. Shahid Zadeh, A. Khooshecharkh, and M. Askari, "Implementation of AI for the prediction of failures of reinforced concrete frames," *International Journal of Reliability, Risk and Safety: Theory and Application*, vol. 5, no. 2, pp. 1–7, 2022, https://doi.org/10.30699/IJRRS.5.2.1.

[32] "ATC-40, Seismic Evaluation and Retrofit of Reinforced Concrete Buildings," Applied Technology Council, California, USA, Rep. SSC 96-01, 1996.

[33] A. Nicknam, M. Khanzadi, S. Motaghed, and A. Yazdani, "Applying b-value variation to seismic hazard analysis using closed-form joint probability distribution," *Journal of Vibroengineering*, vol. 16, no. 3, pp. 1376-1386, 2014.

[34] Z. Karim Zadeh et al., "Development of analytical seismic fragility functions for the common buildings in Iran," *Bulletin of Earthquake Engineering*, vol. 20, no. 11 pp. 5905–5942, 2022, https://doi.org/10/1007/s10518-022-01411-1.

[35] S. Motaghed and A.R. Fakhriyat, "Modeling inelastic behavior of RC adhered shear walls in OpenSees," *Journal of Modeling in Engineering*, vol. 18, no. 63 pp. 15–25, 2021, https://doi.org/10/22059/jmei/.27362.

[36] H. Ghasemi, M. Zare, Y. Fukushima, and K. Koketsu, "An empirical spectral ground-motion model for Iran," *Journal of Seismology*, vol. 13, no. 4, pp. 499–515, 2008, https://doi.org/10.1007/s10950-008-9143-x.

[37] N. Eftekhari, S. Motaghed, L. Emadali, H. Sayyadpour, "Ranking of ground motion prediction equation for use in the seismic hazard analysis of Ahvaz city using data envelopment analysis," *Journal of Engineering Geology,* vol. 16, no. 2, pp. 99–124, 2022.

[38] S. Motaghed, M. Khazaee, and M. Mohammadi, "The b-value estimation based on the artificial statistical method for Iran Kope-Dagh seismic

province," *Arabian Journal of Geosciences*, vol. 14, no. 15, pp. 1–9, 2021, https://doi.org/10.1007/s12517-021-07584-7

[39] S. Akkar and Z. Cagnan, "a local ground-motion predictive model for Turkey, and Its comparison with other regional and global ground-motion models," *Bulletin of the Seismological Society of America*, vol. 100, no. 6, pp. 2978–2995, 2010, https://doi.org/10.1785/0120090367.

[40] S. Akkar, M. A. Sandıkkaya, and J. J. Bommer, "Empirical ground-motion models for point- and extended-source crustal earthquake scenarios in Europe and the Middle East," *Bulletin of Earthquake Engineering*, vol. 12, no. 1, pp. 359–387, 2013, https://doi.org/10.1007/s10518-013-9461-4.

[41] B. J. Chiou and R. R. Youngs, "An NGA model for the average horizontal component of peak ground motion and response spectra," *Earthquake Spectra*, vol. 24, no. 1, pp. 173–215, 2008, https://doi.org/10.1193/1.2894832.

[42] J. X. Zhao, "Attenuation Relations of Strong Ground Motion in Japan Using Site Classification Based on Predominant Period," Bulletin of the Seismological Society of America, vol. 96, no. 3, pp. 898–913, 2006, https://doi.org/10.1785/0120050122.

[43] Task Committee on Blast-Resistant Design of the Petrochemical Committee of the Energy Division of ASCE, *Design of blast-resistant buildings in petrochemical facilities*, 1st ed. American Society of Civil Engineers, 1997.

[44] S. Motaghed and A. R. Fakhriyat, "Modeling inelastic behavior of RC adhered shear walls in OpenSees,"*Journal of Modeling in Engineering*, vol. 18, no. 63, pp. 15-25, 2021, (in Persian), https://doi.org/10.22075/jme.2020.18042.1740.

[45] A. Mehrabi Moghadam, A. Yazdani, and S. Motaghed, "Considering the yielding displacement uncertainty in reliability of mid-rise RC structures," *Journal of Rehabilitation in Civil Engineering*, vol. 10, no. 3, pp. 141–157, 2022, https://doi.org/10.22075/jrce.2021.19660.1376.

[46] S. Motaghed and A. Khooshecharkh, "Probabilistic evaluation of the effects of concrete compression strength on the reinforced concrete building damageability," *European Journal of Scientific Research*, vol. 50, no. 2, pp. 202–207, 2011.

[47] J. W. Baker and C. A. Cornell, "Spectral shape, epsilon and record selection," *Earthquake Engineering & Structural Dynamics*, vol. 35, no. 9, pp. 1077–1095, 2006, https://doi.org/10.1002/eqe.571.